NASA TECHNICAL NOTE

NASA TN D-8083

NASA TN D-8083

DEVELOPMENT AND FLIGHT TESTS OF VORTEX-ATTENUATING SPLINES

Earl C. Hastings, Jr., J. C. Patterson, Jr.,
Robert E. Shanks, Robert A. Champine,
W. Latham Copeland,

Langley Research Center
Hampton, Va. 23665

and Douglas C. Young

Wallops Flight Center
Wallops Island, Va. 23337

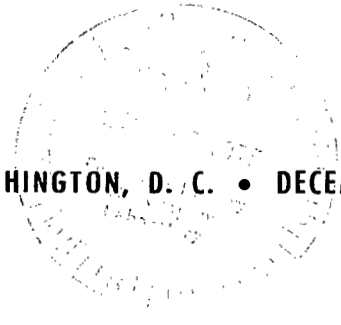

NATIONAL AERONAUTICS AND SPACE ADMINISTRATION • WASHINGTON, D. C. • DECEMBER 1975

1. Report No.	2. Government Accession No.	3. Recipient's Catalog No.
NASA TN D-8083		

4. Title and Subtitle	5. Report Date
DEVELOPMENT AND FLIGHT TESTS OF VORTEX-ATTENUATING SPLINES	December 1975
	6. Performing Organization Code
7. Author(s) Earl C. Hastings, Jr., J. C. Patterson, Jr., Robert E. Shanks, Robert A. Champine, W. Latham Copeland, and Douglas C. Young	8. Performing Organization Report No. L-10442
	10. Work Unit No. 514-52-01-01
9. Performing Organization Name and Address NASA Langley Research Center Hampton, Va. 23665	11. Contract or Grant No.
	13. Type of Report and Period Covered Technical Note
12. Sponsoring Agency Name and Address National Aeronautics and Space Administration Washington, D.C. 20546	14. Sponsoring Agency Code

15. Supplementary Notes

Douglas C. Young is at Wallops Flight Center, Wallops Island, Va.

16. Abstract

This report describes some of the ground tests and full-scale flight tests conducted by the Langley Research Center during development of the vortex-attenuating spline. The flight tests were conducted using a vortex generating aircraft with and without splines; a second aircraft was used to probe the vortices generated in both cases. The results showed that splines significantly reduced the vortex effects, but resulted in some noise and climb performance penalties on the generating aircraft.

17. Key Words (Suggested by Author(s))

Vortices
Vortex attenuation
Flight tests
Full scale
Noise

18. Distribution Statement

Unclassified – Unlimited

Subject Category 02

19. Security Classif. (of this report)	20. Security Classif. (of this page)	21. No. of Pages	22. Price*
Unclassified	Unclassified	39	$3.75

*For sale by the National Technical Information Service, Springfield, Virginia 22161

DEVELOPMENT AND FLIGHT TESTS OF VORTEX-ATTENUATING SPLINES

Earl C. Hastings, Jr., J. C. Patterson, Jr., Robert E. Shanks,
Robert A. Champine, W. Latham Copeland,
Langley Research Center

and Douglas C. Young
Wallops Flight Center

SUMMARY

Flight tests have been conducted to evaluate the spline vortex-attenuation concept developed at the Langley Research Center. An instrumented aircraft was used to probe the vortices of a vortex-generating aircraft (with and without splines) at separation distances between 9.09 km (4.91 n. mi.) and 0.63 km (0.34 n. mi.). The results indicate that the splines significantly reduced the vortex-induced roll acceleration experienced by the probe aircraft, and that the spline made positive roll control possible over the entire range of separation distances.

Installation of splines on the generating aircraft resulted in an appreciable increase in approach noise because of higher required power levels. The rate of climb of the generating aircraft with splines installed was acceptable for these tests although the rate of climb was considerably lower than that of the aircraft without splines. The handling qualities of the generating aircraft were unaffected by the installation of the splines.

INTRODUCTION

The introduction of the wide-bodied jumbo jet into airline service has accentuated the problem of wing-tip vortex effect on aircraft in trail. A number of encounters are on record, and at least one training accident has been attributed directly to the trailing vortex problem. The National Aeronautics and Space Administration (NASA) is engaged in a broad research program to increase understanding of vortex behavior and to develop methods of attenuating the persistence of trailing vortices.

One aspect of this research has been the development of the vortex-attenuating spline concept. Early work on this concept included ground tests in the vortex research facility at Langley Research Center, the Langley VSTOL tunnel, the Hydronautics Corporation towing basin, and full-scale flight tests (refs. 1 to 3).

Initial research in the vortex research facility is briefly described in this paper. The adaptation of the spline concept to a full-scale flight experiment is discussed in detail with concentration on the areas of spline effectiveness as a vortex-dissipation device and to the effects of splines on noise and performance of the generating aircraft.

SYMBOLS

Values are given in both SI and U.S. Customary Units. The measurements and calculations were made in U.S. Customary Units.

p	roll rate, right wing down is positive, deg/sec
$\dot{p}$	roll acceleration, increasing rate is positive, rad/sec^2
$\dot{p}_{a,max}$	maximum aileron-induced roll acceleration in undisturbed air, rad/sec^2
r	yaw rate, nose right is positive, deg/sec
δ	aileron deflection, trailing edge up is positive, deg
ϕ	roll angle, right wing down is positive, deg

Abbreviations:

dB	decibel, unit of measure of sound pressure level $\left(\text{referenced to } 20\ \mu N/m^2\right)$
KIAS	knots indicated airspeed
METO	maximum except take-off engine power
OASPL	overall sound pressure level, dB

APPARATUS AND TEST DESCRIPTION

Vortex Research Facility

The Langley vortex research facility uses the newly developed stationary airflow visualization system, a system based on the fact that air molecules affected by the wing tip of a passing aircraft are set into circular motion with little or no longitudinal flow except for the flow of those air molecules in the vortex core itself. The data discussed here were obtained from tests in a pilot facility (ref. 4) and included the research configurations shown in figure 1. Each test configuration was mounted on a monorail catapult system by a strut that extended out from one wing tip. The catapult propelled the models at a velocity of 24.4 m/sec (80 ft/sec) through a stationary smoke screen used to make the vortices, which were developed by the models, visible. The tests were conducted at a lift coefficient of 0.80. After the models passed through the smoke screen, it was possible to observe the path taken by each vortex, the growth of the vortex core with time, and the interaction of multivortex systems created by various wing-flap settings. The observations were recorded by high-speed cameras throughout the entire lift span of each vortex from the moment the vortex was created until it dissipated.

The basic wing model (fig. 1) had a span of 1.524 m (5.0 ft), a chord of 0.33 m (13 in.), and an NACA 0012 airfoil section. The wing-tip end plates had a circular leading edge with a radius equal to one-fourth the wing chord; the plates extended one-half a chord beyond the wing trailing edge. The distance between the trailing-edge points of the end plates was equal to 1 chord length. The 0.15-m (0.50-ft) diameter flow-through nacelle model was 0.41 m (16 in.) long and was centered on one wing tip to simulate a wing-tip-mounted jet engine. The wing-tip extension had a span of 0.30 m (1 ft) and a chord equal to one-half of the basic wing chord. The extension was mounted so that the leading edge of the extension was at the same chordwise position as in the basic wing model. The parachutes had a diameter equal to 75 percent of the wing chord and were mounted at each wing tip, approximately 1 chord downstream of the wing trailing edge. The spline was a device configured so that each spline blade could be folded about the mounting probe as a method of retraction. The splines ranged from 1/2 to 1 chord length in diameter, and were positioned from the wing quarter chord to $1\frac{1}{2}$ chords behind the trailing edge. The width of each blade was approximately 15 percent of the spline diameter.

Flight Tests

Early tests in the vortex research facility at Langley Research Center and other ground-based facilities indicated that the spline was a promising vortex-attenuation concept. Full-scale flight tests were then conducted with the spline mounted on a generating aircraft to investigate

the effects of splines on the vortex attenuation, noise, and performance. Apparatus and test descriptions of each of these flight investigations are presented in the following sections.

Vortex Attenuation

Since the primary objective of the flight tests was to evaluate the effect of splines on the characteristics of a lift-induced wing vortex, the use of a specific generating aircraft was not deemed critical. Consequently, a four-engine aircraft operated by the Wallops Flight Center was chosen on the basis of immediate availability.

Basic dimensions of the generating aircraft are given in figure 2. Additional characteristics of the test aircraft after modification are given in table I.

For this project, the aircraft was modified as follows:

(1) Spline attachment pods were mounted at each wing tip.

(2) A spline jettison system was installed.

(3) An internal, pressure-fed, vortex visualization system was installed in the aircraft.

(4) A photographic panel consisting of a clock, a vertical speed indicator, an altimeter, and an airspeed indicator was also installed in the aircraft.

Figure 3 is a sketch of the pod-spline assembly. Results of spline tests which were conducted in the pilot LRC vortex research facility (and discussed later in this report) were used to determine the baseline spline dimensions for the flight tests. For this particular generating aircraft, the pod length aft of the tip was 2.08 m (82.0 in.) and the baseline spline diameter was 2.28 m (90 in.). In addition to the 2.28-m (90-in.) diameter spline, a 1.82-m (72-in.) diameter spline was also fabricated and tested to determine whether a 20-percent reduction in the baseline spline diameter adversely affected the vortex-attenuation characteristics.

Tests in the LRC vortex research facility indicated that for a tapered wing such as that on the generating aircraft, the final rolled up position of the vortex system (with flaps up) would be located between 80 percent and 90 percent of the semispan. With flaps down, the vortex location would be further inboard. However, since the extensive structural modifications required to locate the splines inboard precluded anything but a tip-mounted location, the flight tests were made with the splines at the wing tips and with the flaps retracted. In-flight motion pictures showed that this configuration positioned the splines in a location to interact with the tip vortices, even though optimization of the spline location was not possible.

Figure 4 is a photograph of the generating aircraft in flight with the pods and splines attached. A closeup photograph of this assembly is shown in figure 5. The splines for these exploratory tests were not retractable and were attached to the pods by explosive bolts which, in an emergency, could be actuated by the pilot's jettison switch.

A sketch of the vortex visualization system is shown in figure 6. Diatomaceous earth was loaded into each of three hoppers which were manifolded together and mounted to the seat rails in the passenger compartment of the generating aircraft. Four high-pressure nitrogen bottles were used to pressurize the hoppers. The pressure was regulated to 3450 Pa (50 psi) and the downstream side of the regulator had a relief valve as a safety feature. A 2.54-cm (1-in.) discharge tube was routed along the bottom of the right wing and terminated at the end of the pod. Part of the discharge tube can be seen in figure 5.

The vortex probe aircraft used in this project is shown in figures 7 and 8. Pertinent physical characteristics are given in table II. Table III lists the experimental data recorded with the onboard data instrumentation system. For these tests, the following special equipment was installed:

(1) Onboard Distance Measuring Equipment (DME) to display and record the separation distance between the two aircraft

(2) An S-band radar tracking beacon

(3) A fixed, 16-mm motion-picture camera operated by a pilot-controlled switch.

In order to isolate spline effects, it was necessary to maintain constant test conditions to the greatest practical extent. Table IV lists the nominal flight-test conditions and the maximum measured deviations for the tests reported in this report.

On a typical penetration flight, the two aircraft first completed a rendezvous. The desired airspeed, heading, and altitude were established. The probe aircraft records, the DME, and the camera were turned on and the vortex visualization system in the generating aircraft was activated. When the desired separation distance between the two aircraft was established, the probe aircraft approached the vortex trail along a parallel course. Shallow-angle penetrations were then made from just above or below the trail.

Two piloting techniques were used when the vortex was penetrated. To collect data on vortex-induced roll acceleration, the probe aircraft pilot attempted to hold the ailerons neutral, and the aircraft was allowed to roll until thrown out of the vortex. To collect data on roll-control effectiveness, the probe aircraft pilot used the ailerons and tried to maintain a wing-level attitude while in the vortex. Typical time histories of both of these test techniques are shown in figures 9 and 10.

The vortex-induced roll acceleration data $\dot{p}$ presented in this report were determined by taking slopes of the uncorrected roll rate over short time intervals during which the recorded values of aileron deflection were small (illustrated in fig. 9). All values of $\dot{p}$ presented in this report were determined at total aileron deflections of less than 10^{o}.

Noise Measurements

The flight tests for noise measurements were made for two purposes. The first was to assess the aerodynamic noise of the splines by flying the clean airplane (landing gear and flaps

retracted) over the measuring station with the splines off and with the splines on, using the same power settings. For the splines-off case, the flightpath was level; however, for the splines-on case, it was necessary to use a 3° glideslope in lieu of a power increase to compensate for the spline drag. The conditions are given in table V.

The second purpose was to determine the change in landing-approach noise resulting from different power settings for the same approach conditions, namely a 15° flap angle, 110-knot speed, and a 3° glideslope. As shown in table V, the approaches with splines required appreciably more power than those without the splines.

The noise recording station was a self-sufficient mobile van in which the instrumentation necessary for data acquisition was installed. The noise data presented here were measured with a microphone located on the extended center line of runway 10 at the Wallops Flight Center airfield. The microphone was a conventional condenser type with a frequency response flat to within ±2 dB over the frequency range of 5 Hz to 20 kHz. The microphone was positioned 1.5 m (59.1 in.) above ground level with the longitudinal axes parallel to the ground and generally perpendicular to the vertical projection of the flightpath. A wind screen was used at all times. The output of the microphone together with voice and timing signal was recorded on a multichannel frequency-modulated tape recorder located at the measuring station. The entire sound measurement system was calibrated in the field by a conventional discrete-frequency calibrator at the beginning and end of each day of flight tests.

The analog tape recordings obtained during the flight tests were processed through a data reduction and analysis system to compute the overall noise levels, one-third octave band levels, and the effective perceived noise levels. Only the overall sound pressure levels $\left(\text{referenced to } 20\ \mu N/m^2\right)$ are given in this report.

Five noise runs were made for each set of test conditions given in table V. All the runs were made in the same direction and passed over the microphone at an altitude of approximately 114.3 m (375 ft). This nominal test altitude corresponded to that of an aircraft on a 3° glideslope when the aircraft was 1.85 km (1.0 n. mi.) from the runway threshold.

The runs were made visually without electronic guidance, but the aircraft was tracked with radar to determine the actual flightpaths. The aircraft altitude above the microphone for each run was determined from the radar data and then used to correct the overall sound pressure levels to the nominal test altitude.

Generating Aircraft Performance Evaluation

For this flight program special instrumentation for the generating aircraft was limited to four standard cockpit-type instruments (airspeed indicator, altimeter, inertial vertical-speed indicator, and chronometer) mounted in an enclosed, self-illuminated housing installed in the instrument racks of the generating aircraft. Data from these instruments were recorded by a

35-mm camera which photographed the instruments once per second. The special pressure instruments were connected to existing aircraft pitot static system lines.

Other data from the generating aircraft were recorded in flight from standard instruments in the cockpit. Data recorded in this manner included:

(1) Indicated airspeed and vertical speed for backup rate-of-climb data

(2) Manifold pressure, engine revolutions per minute (rpm), and carburetor air temperatures for determination of brake horsepower from engine calibration curves.

A typical performance test sequence was as follows:

(1) If splines were installed, a dive test was conducted through a range of airspeeds up to the limit value defined by the "splines on" structural analysis. The purpose of the test was to verify wing-spline structural integrity and to determine if deleterious flutter or vibration existed in the test speed range.

(2) Power-off stall tests to onset of buffet for the clean configuration and the take-off configuration were made.

(3) Four-engine rate-of-climb checks were made at 10 KIAS increments from 100 KIAS to maximum straight and level airspeed at maximum power in the take-off configuration.

(4) Four-engine and simulated three-engine rate-of-climb checks were made at 10 KIAS increments from 100 KIAS to maximum straight and level airspeed at METO power in the clean configuration.

Climb tests were accomplished by attaining a stable rate of climb at a constant airspeed, and data were recorded for a 60-sec period during the climb. For a given configuration, the climb-test sequence became a set of sawtooth climbs with the airspeed of the recorded ascent increasing at 10 KIAS increments.

Atmospheric data for performance flights were determined from Weather Bureau records. Weight (mass) data were derived from basic weight and balance data and from fuel measurements taken before and after each flight.

After each flight, the film records were analyzed to determine stall airspeed and rate of climb. The stall airspeed was taken at the instant when the vertical speed increased sharply. The calibrated airspeed was taken from cockpit airspeed calibration placards and from reference 3.

In this report, "predicted" and "flight test" rate-of-climb data are given. "Predicted" values were derived by taking measured data for the generating aircraft without splines; normalizing these data to a mass of 24 970 kg (55 000 lbm), sea level, and standard day; and adding flat-plate spline profile drag to predict the spline effect. The normalization required construction of a drag polar using measured rate-of-climb data and (since engine performance

was not measured) engine calibration curves from reference 4. Data labeled "flight tests" were taken directly from recorded rate-of-climb measurements normalized in the same manner.

TEST RESULTS

LRC Vortex Research Facility Test

With the basic wing panel in the test facility, visual data showed that the tip vortices moved downward and inward toward the vertical plane of symmetry under the influence of the wing downwash. Because of centrifugal forces associated with rotational flow, each vortex core formed a distinct void in the smoke screen. Smoke was also observed moving upstream along the periphery of the vortex core. This feature of the flow-visualization method allowed a three-dimensional view of the vortex so that the variation in core size could be seen along the path of the model. The meander and the persistence of the vortices of the basic wing were obvious from these tests as was the spanwise movement of the vortices as they approached the ground.

End plates were mounted at each wing tip as a first attempt to interrupt the vortex development process. Visually, it was possible to detect a slight delay in the formation of the vortex which appeared a short distance downstream of the end plate; this vortex was qualitatively as strong as the basic wing vortex with no change in persistence. This separation between the wing trailing edge and the position where the vortex did form may account for the well-known decrease in induced drag associated with wing tip end plates.

The tip-mounted flow-through nacelle (or ring end plate) was also tested in an effort to reduce the strength of the vortex. Although no flow measurements were made, it was assumed that there was very little blockage of the nacelle flow at the test velocity. Here again there was a delay in the vortex formation; this delay was followed shortly by a tightly wound vortex.

As a third attempt to introduce a change in the wake of the basic wing panel, a wing-tip extension was attached to one wing tip. This change in wing planform was proposed to alter the wing span loading in order to produce two vortices. Such an alteration would tend to reduce the energy level of each vortex because of their proximity and possibly their same sense of rotation. Two vortices were formed which rotated in a helix about a central axis and merged into one vortex similar to the vortex produced by one wing tip of the basic wing panel.

In studying these visual data, in addition to data from a number of other configurations, it became apparent that the vortex could not be eliminated or attenuated by merely reshaping the wing tip. A change in tip configuration may affect the near-field vortex but produce only a small effect on the far-field flow. It was therefore considered no solution to the vortex persistence problem. A concept was then developed to introduce an unfavorable or positive

pressure gradient just downstream of the wing tip to force the vortex to dissipate. This was accomplished by employing a parachute at each wing tip. Flow visualization tests showed that the vortex was virtually eliminated by this procedure in both the near and far fields. The success of this concept is believed to result from the shearing stresses existing between the rotational vortex flow and the linear flow of the mass of air forced into each vortex core by the parachutes. As an alternate application of this concept, a number of splines were probe mounted just downstream of each wing tip. Visualization flow tests using this configuration indicated the same results as those obtained using the parachute.

Evaluation of the visual data from the spline tests and performance estimates indicated that a spline having a diameter of 55 percent of the chord length and mounted 50 percent of the chord length behind the wing trailing edge would produce significant vortex attenuation without an excessive drag penalty. These dimensions were used in the flight test for the baseline spline.

Flight Tests

The following sections present the results of the flight tests for vortex attenuation, noise measurements, and generating aircraft performance evaluation.

Vortex Attenuation

In this report, the effects of splines on the vortex of the generating aircraft are presented in terms of two parameters: the vortex-induced roll acceleration $\dot{p}$ on the penetrating aircraft with neutral (or nearly neutral) ailerons and the separation distance at which the full aileron throw of the penetrating aircraft was insufficient to overcome vortex-induced roll velocity. The first parameter is important since it is an indication of vortex-induced rolling moments (as opposed to aileron-induced rolling moments). The roll-control separation distance is important because it relates to the ability of the following pilot to recover from a vortex encounter.

In this report, values of roll acceleration measured during vortex penetrations with ailerons neutral are normalized to the maximum roll acceleration produced by the ailerons (at full throw) in undisturbed air. (For this probe aircraft at an altitude of 2134 m (7000 ft) and an indicated airspeed of 90 knots (1 knot = 0.5144 m/sec), the value of $\dot{p}_{a,max}$ from test data was 2.68 rad/sec^2.) This ratio is not related to the controllability of the probe aircraft, but is intended as an index for evaluating the vortex effect. (That is, values of $\dot{p}/\dot{p}_{a,max} > 1.0$ indicate that the rolling accelerations experienced during penetrations with neutral ailerons are larger than the maximum rolling accelerations which the ailerons could produce in undisturbed air.) Data are shown as a function of separation distance in figure 11 for splines off and with the 1.82-m (72-in.) and 2.28-m (90-in.) splines installed.

The collected test data showed a great deal of scatter caused by variations of the probe aircraft position in the vortex and by deviations in nominal test conditions. Consequently, only those points having the larger values are shown in figure 11. The solid and broken lines show the upper boundaries of all the data collected. Since the test data upper boundary with both the 1.82-m (72-in.) and 2.28-m (90-in.) diameter splines were so nearly the same, these data are treated as one curve in this figure.

The data show that the vortex-induced roll without splines increased rapidly as separation distance was shortened from 9.09 km (4.91 n. mi.) to 5.39 km (2.91 n. mi.). At separation distances less than 7.20 km (3.89 n. mi.), the vortex-induced roll acceleration was larger than the maximum aileron-induced roll acceleration in undisturbed air. Penetrations of the unattenuated vortex were not made closer than 3.70 km (2.00 n. mi.) because the pilot of the probe aircraft felt the upset might cause structural damage. With either the 1.82-m (72-in.) diameter or the 2.28-m (90-in.) diameter splines installed on the generating aircraft, the vortex-induced roll was generally 40 percent to 50 percent of the maximum aileron-induced value, and penetrations were made safely as close as 0.63 km (0.34 n. mi.). No change in the spline attenuation characteristics because of the 20-percent decrease in diameter could be determined from the flight-test data collected.

The effect of the 2.28-m (90-in.) diameter spline on the roll-control capability of the probe aircraft using ailerons is shown in figures 12 and 13. Figure 12 is the recorded time history of penetrations of the unattenuated vortex at 4.06 km (2.19 n. mi.) behind the generating aircraft. It can be seen that between 12 sec and 13 sec, with the ailerons fully deflected to produce a positive roll to the right, the aircraft was actually rolling to the left. The same effect can be seen between 28 sec and 30 sec. Here, with the ailerons again fully deflected for a right-hand roll, the aircraft was overpowered by the vortex and was rolling to the left. These results indicated that with no splines installed on the generating aircraft, the roll control of the probe aircraft was overpowered by the vortex at this distance.

Data recorded during penetration of the attenuated (splines on) vortex at 1.56 km (0.84 n. mi.) are shown in figure 13. These data show that the roll control of the probe aircraft was positive at this distance and required only about 25 percent of the total aileron deflection available. Other recorded data (not presented) show the same effect at separation distances as close as 1.14 km (0.62 n. mi.). These results are supported by the test pilot's assessment that without attenuation, roll control became insufficient at about 4.63 km (2.50 n. mi.); with attenuation (either by 1.82-m (72-in.) or 2.28-m (90-in.) diameter splines), roll control was positive through the entire range of separation distances.

Noise Measurements

The noise measurement results obtained during the tests are presented in figures 14 and 15 in the form of typical noise time histories and noise spectra, respectively. In addition,

maximum noise values for overall sound pressure levels (corrected to an altitude of 114.3 m (375.7 ft)) and effective perceived noise levels are given in table VI for all the test runs. These values are summarized in table VII as averages for the five runs for each condition. The atmospheric conditions prevailing during the flights are given in table VIII.

Typical time histories of overall sound pressure levels for the generating aircraft with and without splines are shown in figure 14. Data from the constant power flybys (aircraft with gear and flaps retracted) are given in figure 14(a) and data from the landing approaches (aircraft with gear down and 15^{o} flap angle) are given in figure 14(b). These time histories were plotted from flyover data obtained at the 1/2-sec sampling rate. The zero on the time scale corresponds to the time at which the airplane is directly over the noise measuring station.

Figure 14(a) shows that the noise levels for the flyby reach a maximum approximately 3 sec before the airplane is directly over the noise measuring station for both conditions (with and without splines). Similar results are shown in figure 14(b) for the landing-approach configuration operations with maximum noise levels occurring approximately 5 sec before the airplane is directly over the noise measuring station.

The data in table VII for the constant power flybys show that the corrected overall sound pressure levels are virtually the same for the airplane with and without splines. Comparison of the results for the landing approaches given in this same table, however, shows that the splines resulted in appreciably higher noise (approximately 4 dB) for the corrected overall sound pressure level. This difference is attributed to the higher engine power conditions required to overcome the drag of the splines. (See table V.)

Generating Aircraft Performance Evaluation

Results of this evaluation are given in terms of the effects of splines on:

(1) Power-off stall speed: take-off and clean configurations

(2) Rate of climb: take-off configuration using maximum power

(3) Rate of climb: clean configuration using METO power.

Power-off stall speeds.- The results of the measured power-off stall speeds and values predicted from reference 5 are listed in table IX. Stall speeds for the clean configuration (flaps up) and for the take-off configuration (15^{o} flaps) are normal. The splines do not appear to alter the generating aircraft stall airspeeds. Minor differences between the measured values and those of reference 5 can be attributed to errors in chart interpolation, instrument indications, and pilot technique.

Rate of climb: take-off configuration and maximum power.- Predicted and flight-test data are shown in figure 15 for the generating aircraft with and without splines for the take-off configuration (gear down, flaps 15^{o}) with four engines at maximum power. For

consistency, all test data are normalized to a mass of 24 970 kg (55 000 lbm) at sea level on a standard day. The figure shows excellent agreement between predicted and test data. The rate of climb with the 2.28-m (90-in.) diameter splines is 215 m/min (704 ft/min) at 110 knots and 140 m/min (460 ft/min) at 120 knots. Values for the 1.82-m (72-in.) diameter splines are about 50 m/min (164 ft/min) higher in this speed range. For these tests, the minimum acceptable rate of climb was arbitrarily taken as 61 m/min (200 ft/min) on the basis of pilot recommendations. Using these criteria, acceptable rates of climb with the 2.28-m (90-in.) diameter splines are available up to an airspeed of about 128 knots in the take-off configuration with four engines operating.

Although three-engine tests were not performed with the take-off configuration, predictions of rate of climb were made. The four-engine test data from figure 15 were adjusted for a 25-percent reduction in available power and the addition of windmilling propeller drag from reference 5. The calculations indicated that with either size spline installed, the rate of climb was unacceptable for this condition. Because of the spline jettison feature, however, this situation was hazardous only if an engine failure and a spline jettison failure occurred simultaneously.

Rate of climb: clean aircraft with METO power.- Figure 16 presents predicted and test data for the clean (flaps up, gear up) configuration with four engines with and without splines. At 110 knots, the test data are 296 m/min (970 ft/min) and 270 m/min (885 ft/min) for the 1.82-m (72-in.) and 2.28-m (90-in.) splines, respectively. At 130 knots, test data are 214 m/min (700 ft/min) and 153 m/min (500 ft/min) for the 1.82-m (72-in.) and 2.28-m (90-in.) splines, respectively.

Comparison of predicted and test data for this configuration, unlike the preceding flaps 15° case (where agreement was good), shows that the spline effect is overpredicted at the lower airspeeds. Although limited test instrumentation in the generating aircraft precluded a rigorous analysis of this effect, it may result from uncertainties in available power, or from reduced generating aircraft drag due to lift with splines installed.

Data for the clean configuration with and without splines are shown in figure 17 for three-engine performance. Test data were based on flight tests with a simulated engine-out feathered-propeller situation. The figure shows that although predicted rate-of-climb values were unacceptable, the flight-test results indicated acceptable values for both size splines up to 120 knots indicated airspeed. It is apparent here, as in the four-engine case, that the actual rate of climb was better than the predicted rate of climb determined by adding spline drag to the basic generating aircraft flight-test data.

All of the performance-test results with splines on show essentially the same result: splines significantly reduce the available rate of climb. However, for all cases except the three-engine take-off configuration, an acceptable rate of climb was possible with the splines for the test weight used in the program. The pilots of the generating aircraft observed that

handling qualities were not noticeably changed by the installation of the splines, regardless of spline size or aircraft configuration. Spline-induced flutter or vibration was not evident on any of the test flights.

CONCLUDING REMARKS

The results of flight tests conducted to determine the ability of wing-mounted splines to attenuate trailing vortices indicated the following:

1. Penetrations of the unattenuated vortex at distances closer than 7.20 km (3.89 n. mi.) resulted in roll accelerations larger than the maximum aileron-induced value. With splines on, the vortex-induced roll acceleration was reduced to about 50 percent of the aileron-induced roll over the range of separation distances tested (9.1 km (4.9 n. mi.) to 0.62 km (0.33 n. mi.)).

2. When the unattenuated vortex was probed at distances closer than about 4.6 km (2.5 n. mi.), the ailerons of the probe aircraft could not overcome the vortex-induced roll. With splines on, positive roll control was available at separation distances as close as 1.14 km (0.62 n. mi.).

3. The maximum overall sound pressure level of the generating aircraft during landing approach with splines on was approximately 4 dB higher than with the splines off.

4. Although splines significantly reduced the rate of climb of the generating aircraft, the four-engine performance was acceptable for this test program.

5. The splines caused no noticeable changes in the handling qualities of the generating aircraft.

Langley Research Center
National Aeronautics and Space Administration
Hampton, Va. 23665
September 29, 1975

REFERENCES

1. Patterson, James C., Jr.: Lift-Induced Wing-Tip Vortex Attenuation. AIAA Paper No. 74-38, Jan.-Feb. 1974.
2. Kirkman, Karl L.; Brown, Clinton E.; and Goodman, Alex: Evaluation of Effectiveness of Various Devices for Attenuation of Trailing Vortices Based on Model Tests in a Large Towing Basin. NASA CR-2202, 1973.
3. Hastings, Earl C., Jr.; Shanks, Robert E.; Champine, Robert A.; Copeland, W. Latham; and Young, Douglas C.: Preliminary Results of Flight Tests of Vortex Attenuating Splines. NASA TM X-71928, 1974.
4. Patterson, James C., Jr.; and Jordan, Frank L., Jr.: A Static-Air Flow Visualization Method To Obtain a Time History of the Lift-Induced Vortex and Circulation. NASA TM X-72769, 1975.
5. Flight Manual: USAF Series C-54, EC-54, HC-54, and TC-54; Navy Models C-54 (R5D). USAF T.O. 1C-54D-1; NAVWEPS 01-4ONS-1, Aug. 30, 1963.

TABLE I.- CHARACTERISTICS OF THE GENERATING AIRCRAFT

Empty operational mass, kg (lbm)	22 294 (49 150)
Wing area, m^2 (ft^2)	135.8 (1462.0)
Wing mean aerodynamic chord, m (ft)	4 (13.61)
Wing aspect ratio	9.44
Wing incidence (root), deg	4
Wing incidence (tip), deg	1
Horizontal tail area, m^2 (ft^2)	30.2 (324.9)
Vertical tail area, m^2 (ft^2)	16.7 (179.3)
Engine	Pratt and Whitney 2000 D-5
Propeller data:	
Type	Hamilton standard constant speed
Gear ratio	2:1
Blade activity factor	100
Diameter, m (ft)	3.97 (13.0)

TABLE II.- CHARACTERISTICS OF THE PROBE AIRCRAFT

Mass:	
Empty operational, kg (lbm)	799 (1761)
Gross take-off, kg (lbm)	1009 (2225)
Roll moment of inertia (approximate):	
At empty mass, kg-m^2 $(slug\text{-}ft^2)$	1085 (800)
At gross take-off mass, kg-m^2 $(slug\text{-}ft^2)$	1627 (1200)
Wing data:	
Area, m^2 (ft^2)	14.9 (160)
Span, m (ft)	9.14 (30)
Chord, m (ft)	1.6 (5.3)
Aileron data (each):	
Span, m (ft)	1.6 (5.3)
Chord, m (ft)	0.305 (1.0)
Engine type	Lycoming 0-360-A3A
Propeller data:	
Type	Sensenich M76EMMS (fixed pitch)
Diameter, m (ft)	1.9 (6.3)

TABLE III.- PROBE AIRCRAFT INSTRUMENTATION

Roll rate
Yaw rate
Pitch rate
Lateral acceleration
Normal acceleration
Longitudinal acceleration
Roll attitude
Pitch attitude
Angle of attack
Angle of sideslip
Aileron position (left)
Aileron position (right)
Rudder position
Stabilator position
Flap position
Throttle position
Heading
Airspeed (indicated)
Altitude

TABLE IV.- NOMINAL TEST CONDITIONS FOR VORTEX PENETRATIONS

Parameter	Nominal condition	Measured deviation
Generating aircraft mass	24 970 kg (55 000 lb)	-227; 454 kg (-500; 1000 lb)
Generating aircraft airspeed, indicated	115 knots	±3 knots
Probe aircraft mass	950 kg (2093 lb)	±60 kg (±132 lb)
Probe aircraft penetration airspeed, indicated	90 knots	±10 knots
Test altitude	2134 m (7000 ft)	-------

TABLE V.- NOISE TEST CONDITIONS

Flight conditions			Engine conditions		
	Splines	Glidepath, deg	Manifold pressure, Pa (in. Hg)	rpm	Engine power, kW, (bhp)
Flyby: gear and flaps retracted, 115 KIAS	Off	0	87 799 (26)	2115	439.9 (590)
	On	3	87 799 (26)	2115	439.9 (590)
Landing approach: gear down, 110 KIAS	Off	3	74 292 (22)	2300	354.2 (475)
	On	3	101 307 (30)	2300	600.3 (805)

TABLE VI.- MAXIMUM NOISE VALUES DURING FLYBY AND APPROACH OPERATIONS WITH AND WITHOUT 2.28-m (90-in.) DIAMETER SPLINES

(a) Flyby: gear and flaps retracted, 115 KIAS

Run	Without splines		With splines	
	OASPL, dB		OASPL, dB	
	Measured	Corrected	Measured	Corrected
1	103	104	107	104
2	103	104	104	102
3	102	104	103	102
4	101	100	103	102
5	104	105	105	105

(b) Landing approach: gear down, flaps 15°, 110 KIAS

Run	Without splines		With splines	
	OASPL, dB		OASPL, dB	
	Measured	Corrected	Measured	Corrected
1	102	102	106	105
2	103	101	107	107
3	100	101	104	105
4	103	102	106	106
5	99	100	106	105

TABLE VII.- SUMMARY OF SOUND MEASUREMENT RESULTS

Flight condition	OASPL, dB		
	Splines		Difference
	Off	On	
Flyby: gear and flaps retracted, 115 KIAS	103.4	103.0	0.4
Landing approach: gear down, flaps 15°, 110 KIAS	101.2	105.6	4.4

TABLE VIII.- SURFACE AND UPPER AIR ATMOSPHERIC CONDITIONS FOR TEST PERIODS

Date	Upper air data									Surface winds		
	Altitude		Atmospheric pressure		Temperature		Relative humidity, percent	Wind velocity knots	Wind direction, deg	Time of day	Velocity, knots	Direction, deg
	m	ft	Pa	lb/ft^2	K	^oF						
12-6-73	4	13	101 410	2118	285	53	83	10	270	0800	9	320
0722 EST	121	397	100 000	2089	285	53	80					330
	273	895	98 200	2051	285	53	76	20	304	0900	9	330
	797	2614	92 200	1926	280	45	100	16	297			
12-7-73	4	13	102 800	2147	276	38	66	10	340	0800	4	345
0740 EST	228	748	100 000	2089	276	37	45	25	355			
	607	1991	95 400	1992	273	32	50	23	346	0900	9	350

TABLE IX.- GENERATING AIRCRAFT STALL SPEEDS (POWER OFF) WITH AND WITHOUT SPLINES

	Take-off configuration			Clean configuration		
	Mass, kg (lbm)	Measured stall speed, KIAS	Predicted stall speed, KIAS	Mass, kg (lbm)	Measured stall speed, KIAS	Predicted stall speed, KIAS
No splines	24 766 (54 600)	79	77	24 312 (53 600)	92	88
1.82-m (72-in.) splines	24 698 (54 450)	79	77 (No splines)	24 743 (54 550)	91	89 (No splines)
2.28-m (90-in.) splines	25 220 (55 600)	80	78 (No splines)	25 174 (55 500)	94	90 (No splines)

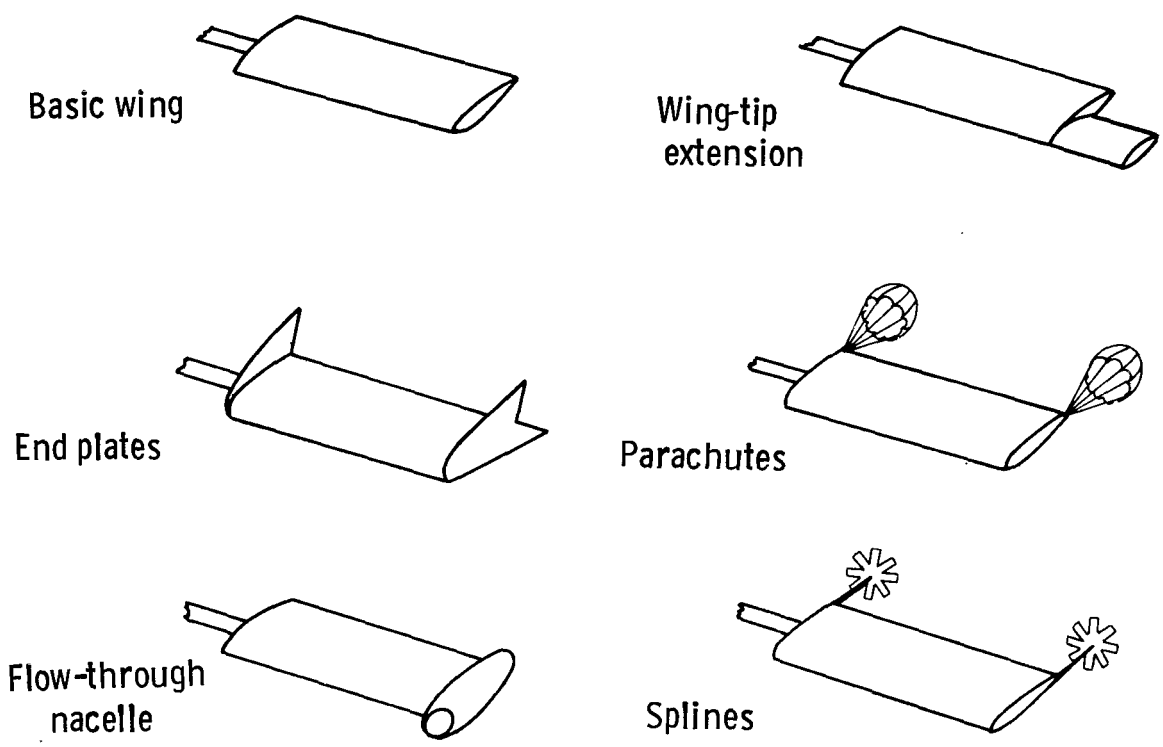

Figure 1.- Vortex-attenuation configurations.

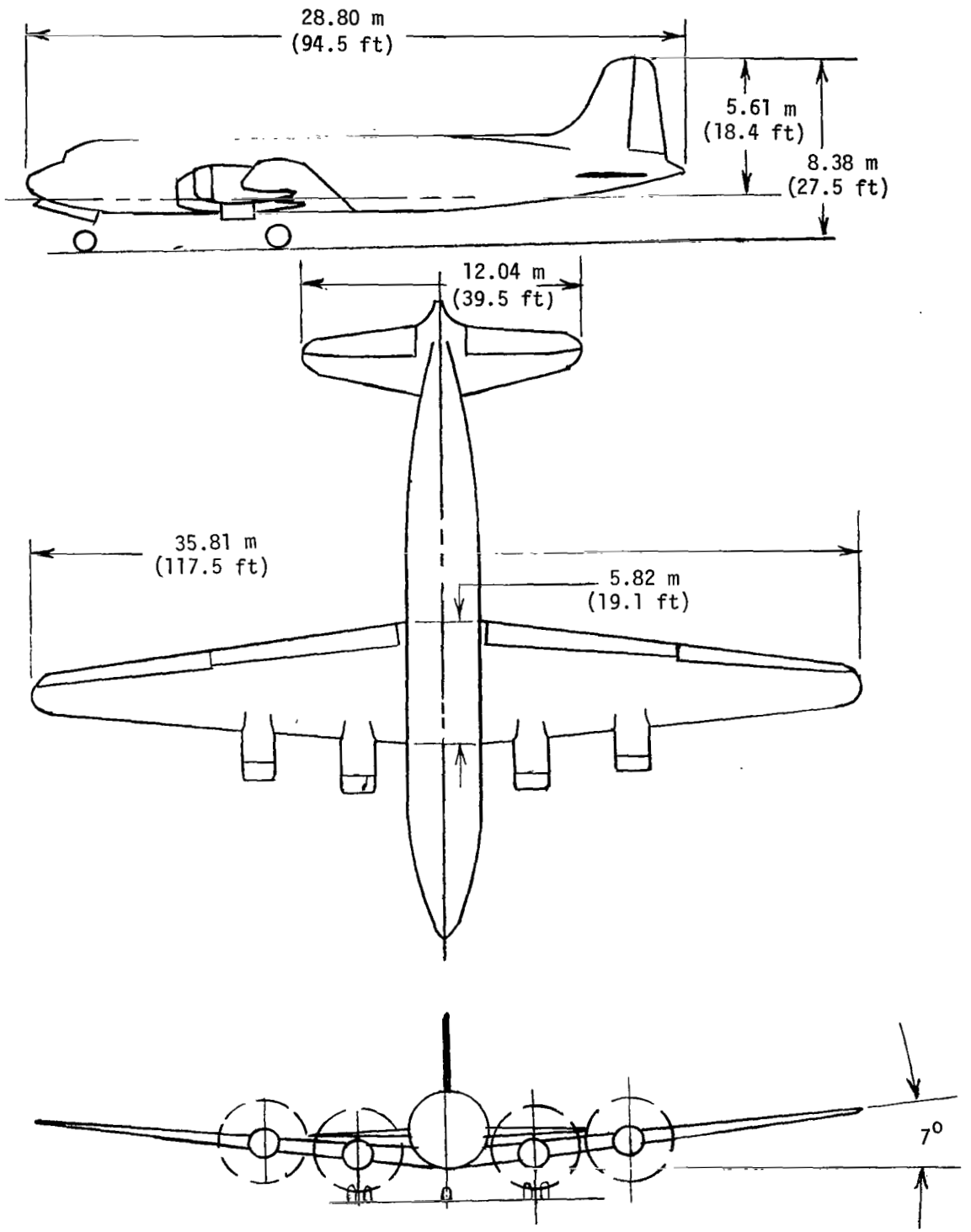

Figure 2.- Diagram of unmodified generating aircraft.

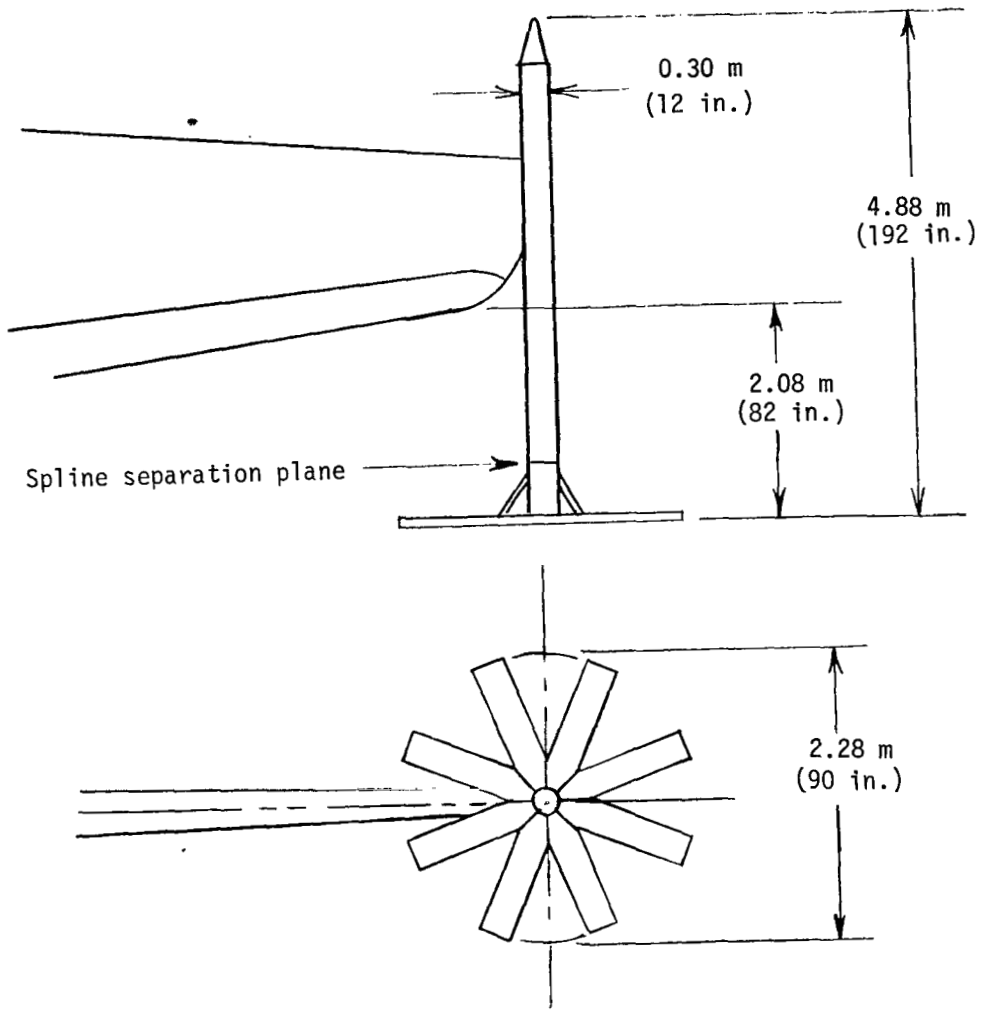

Figure 3.- Sketch of spline assembly at wing tip.

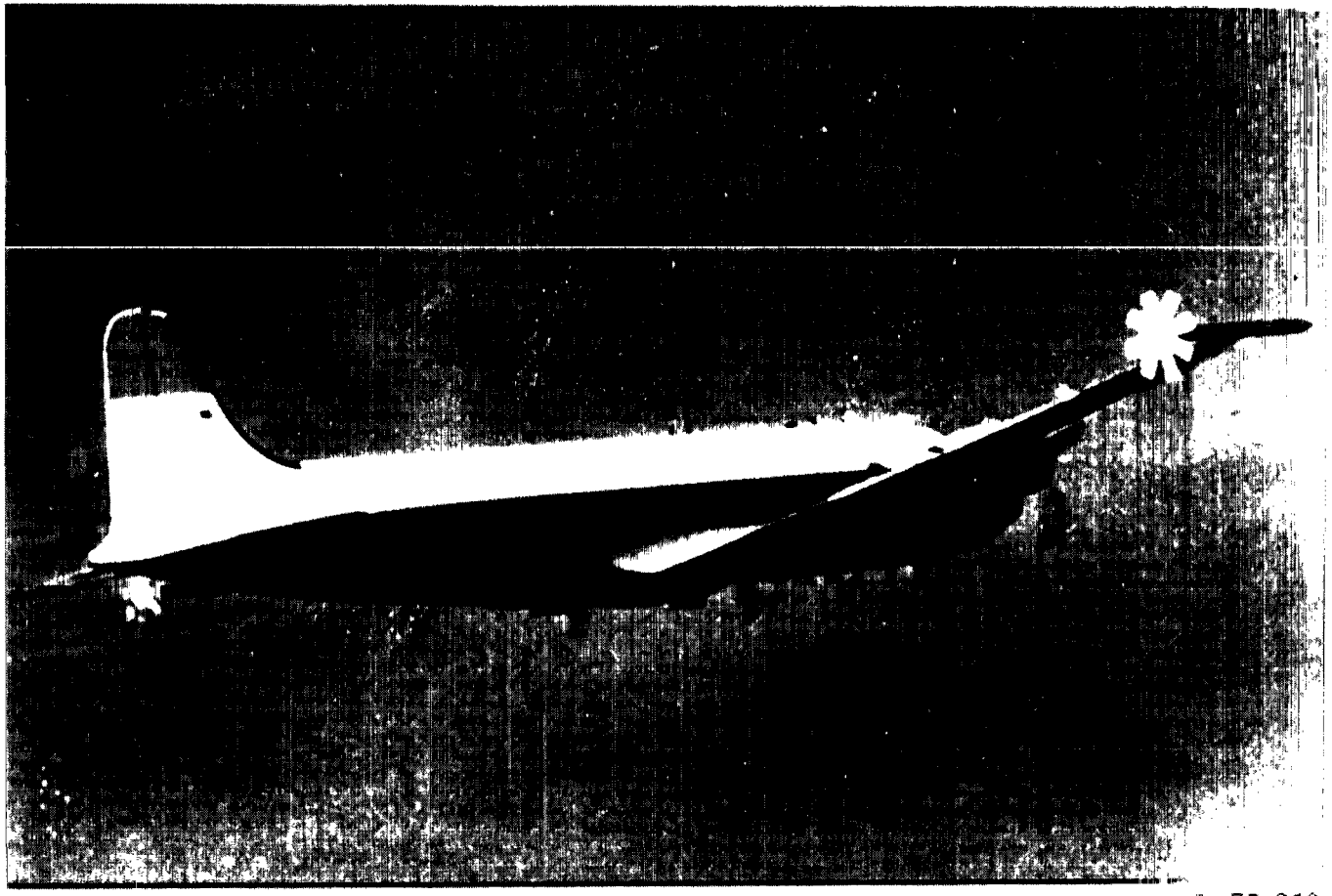

L-75-219

Figure 4.- Generating aircraft with splines attached.

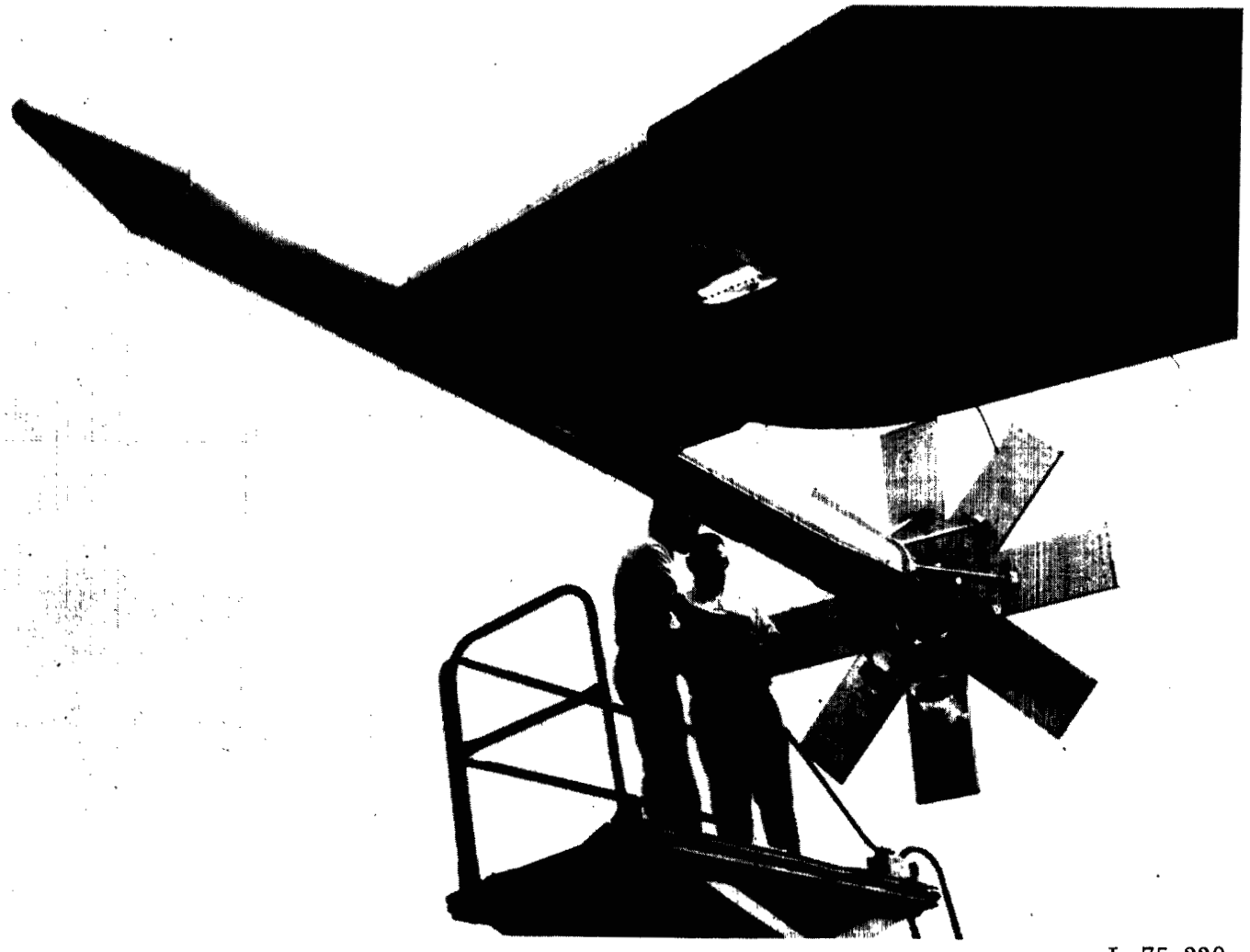

L-75-220

Figure 5.- Pod-spline assembly on wing tip of generating aircraft.

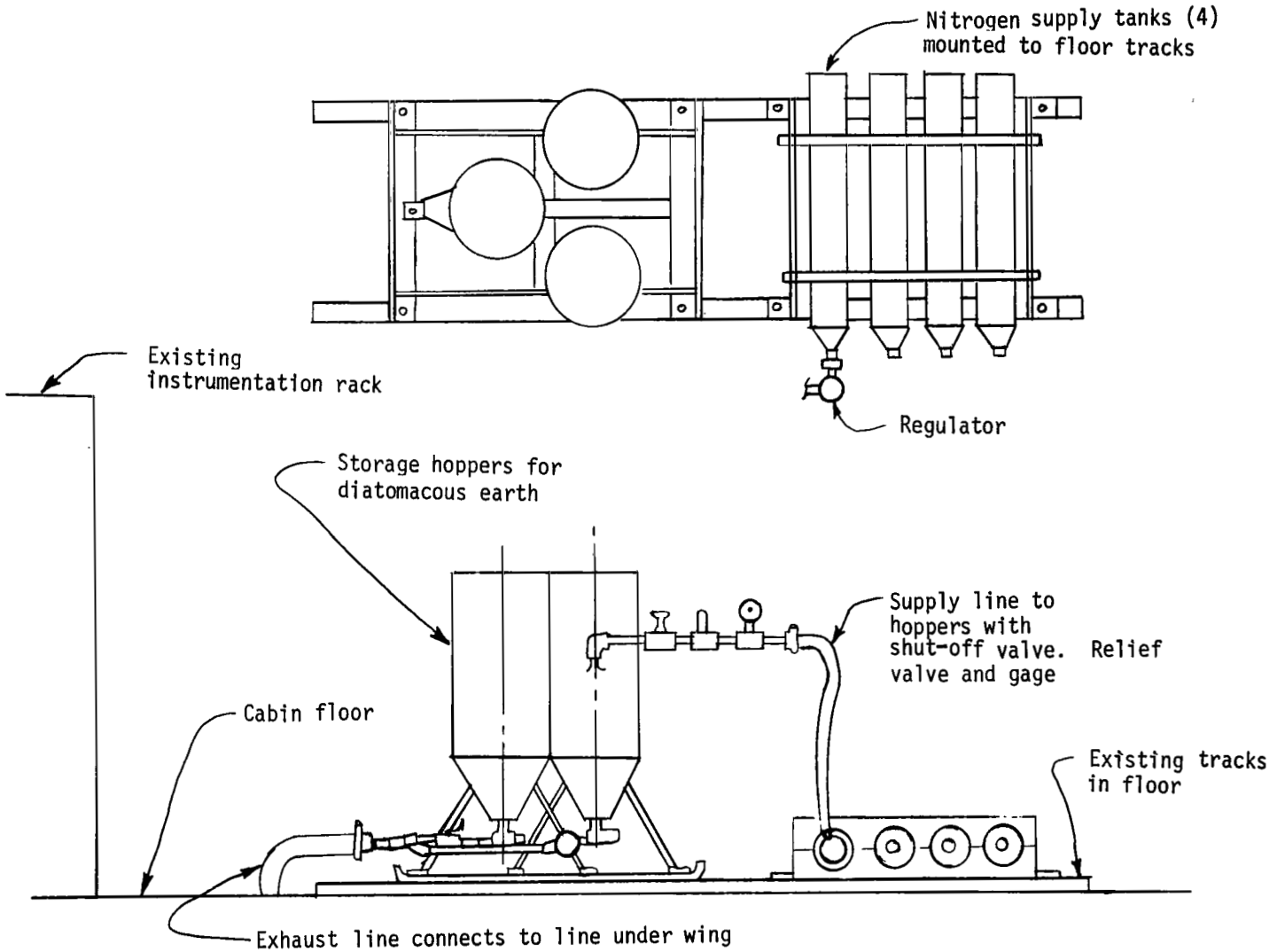

Figure 6.- Diagram of vortex visualization system.

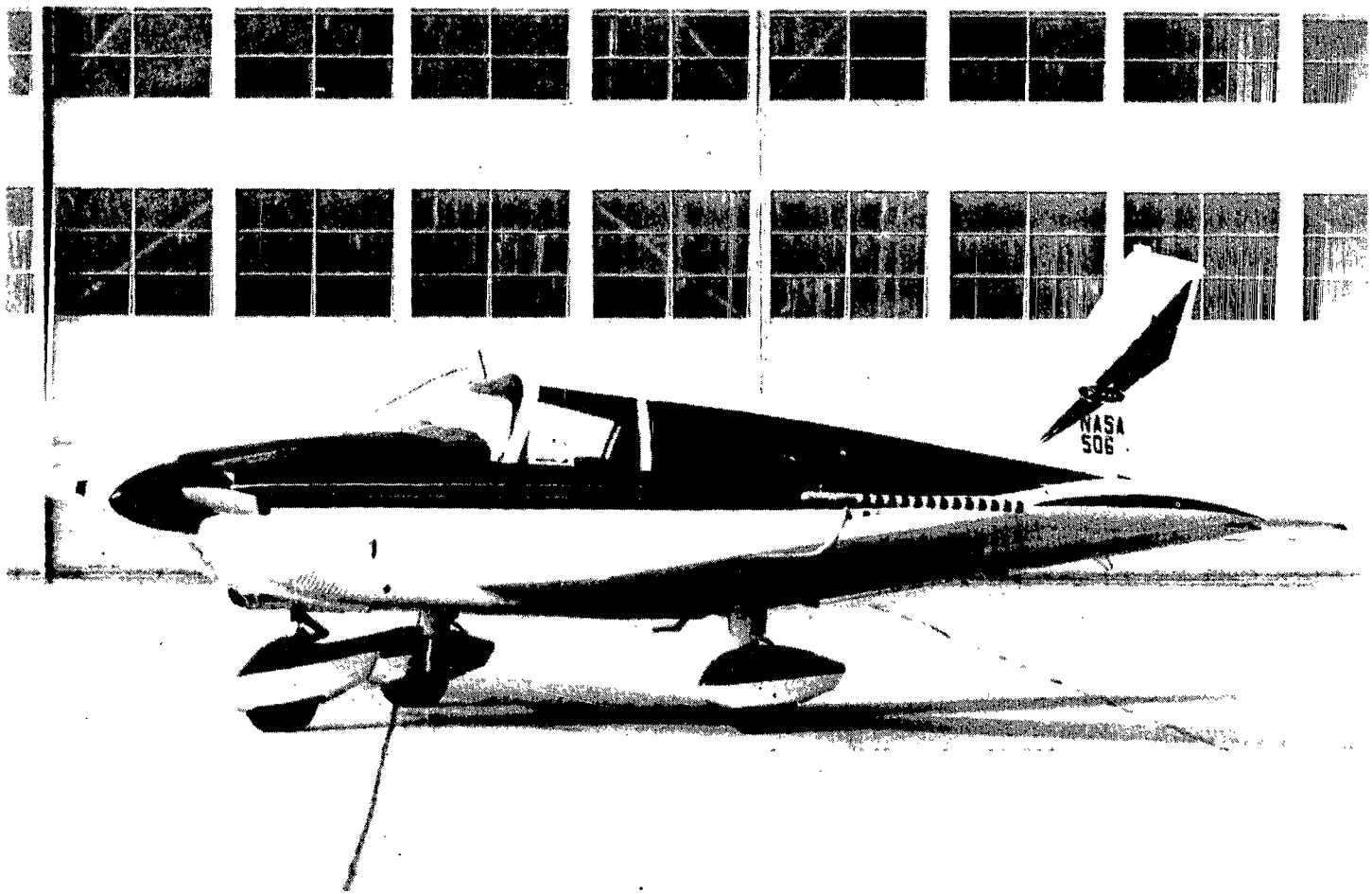

L-75-221

Figure 7.- Photograph of probe aircraft.

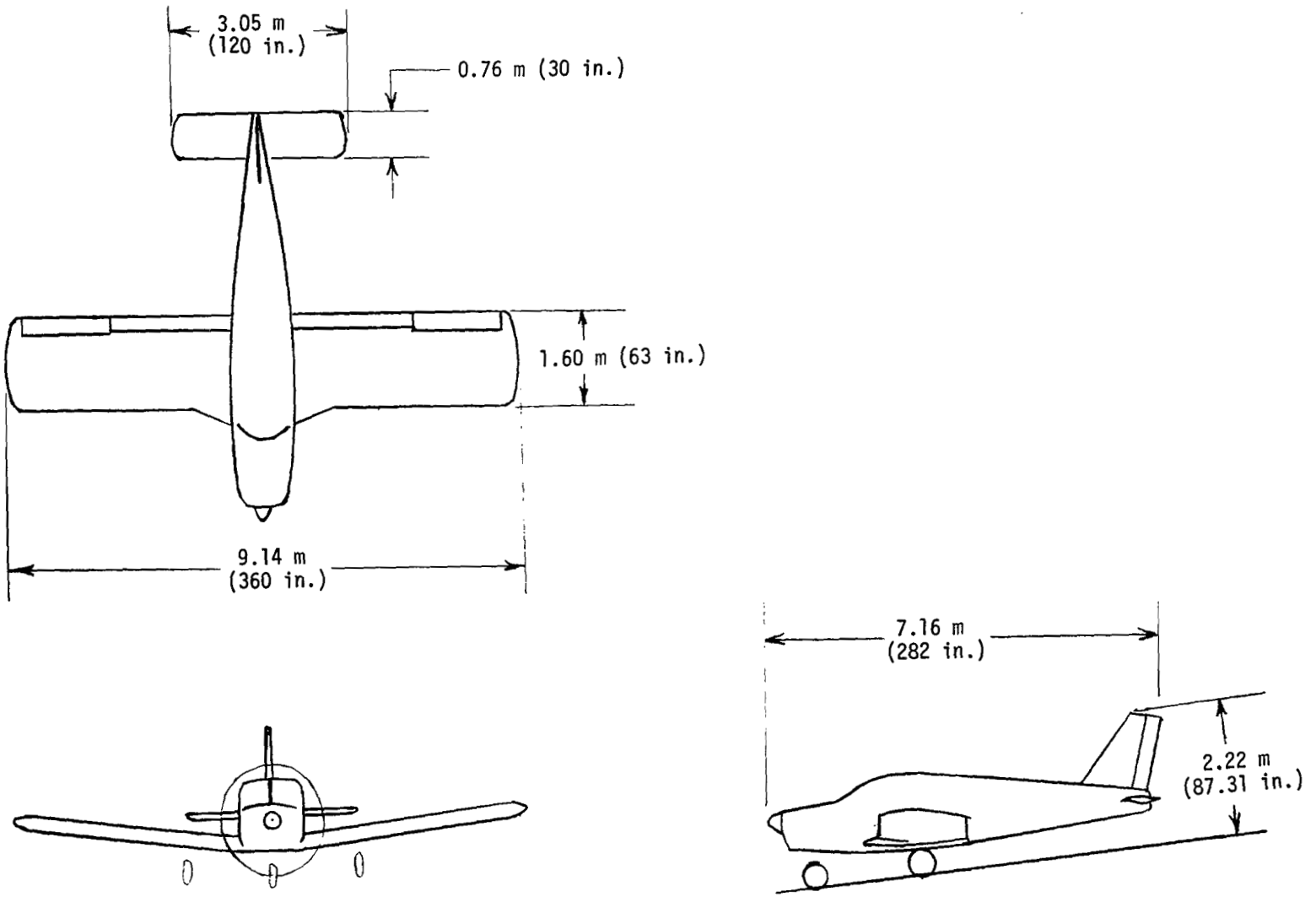

Figure 8.- Diagram of probe aircraft.

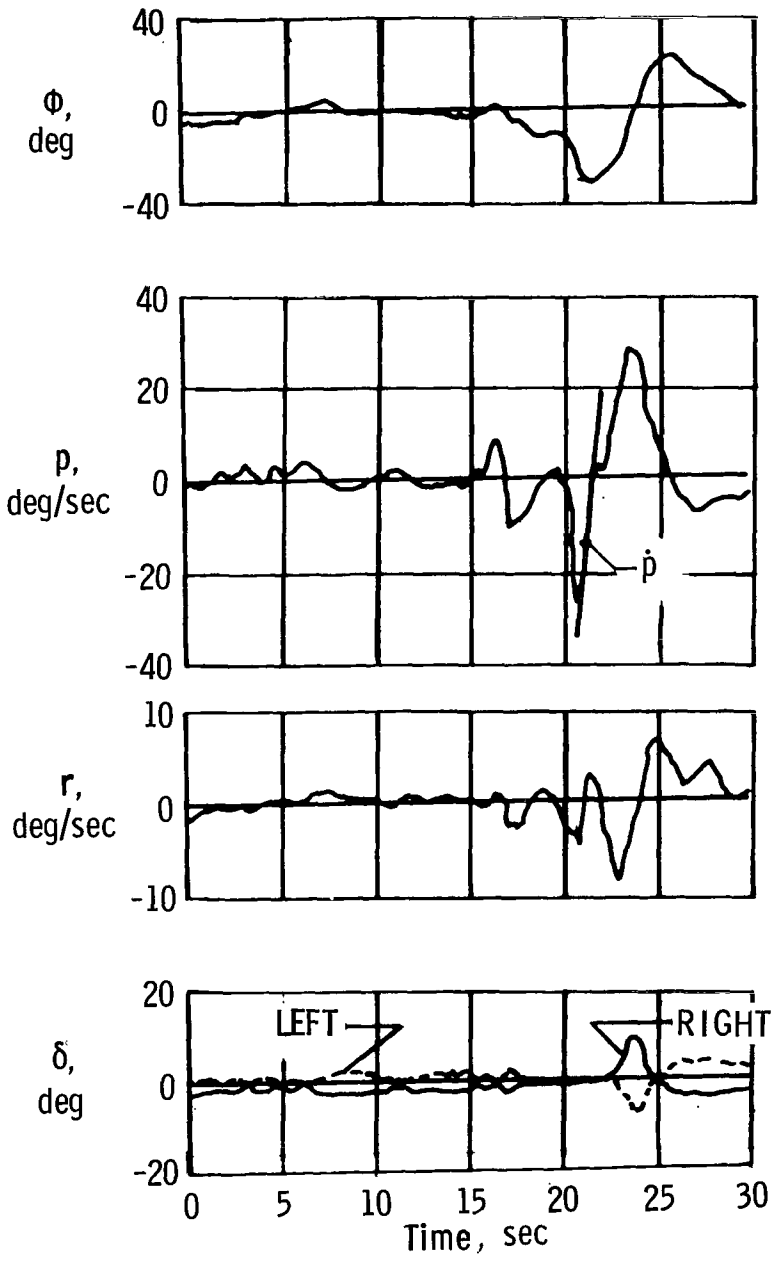

Figure 9.- Typical time history of penetrations with ailerons neutral.

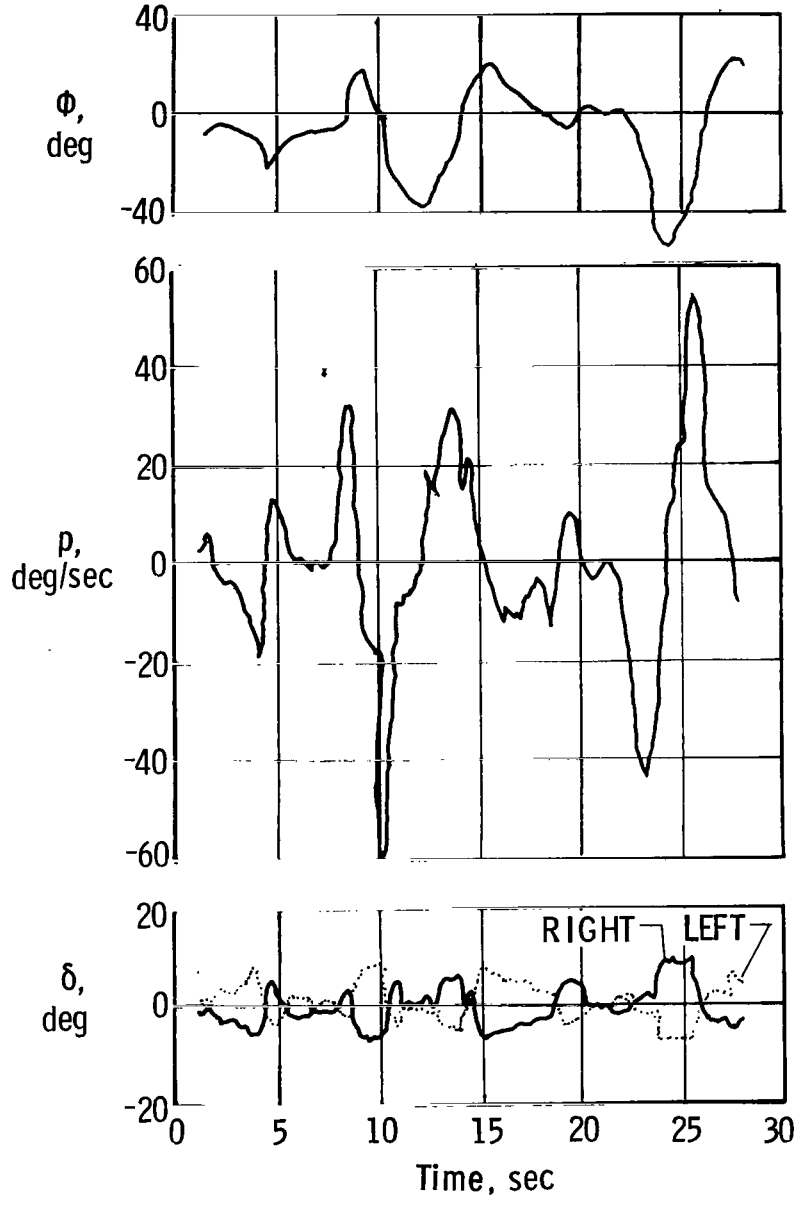

Figure 10.- Typical time history of penetrations with ailerons active.

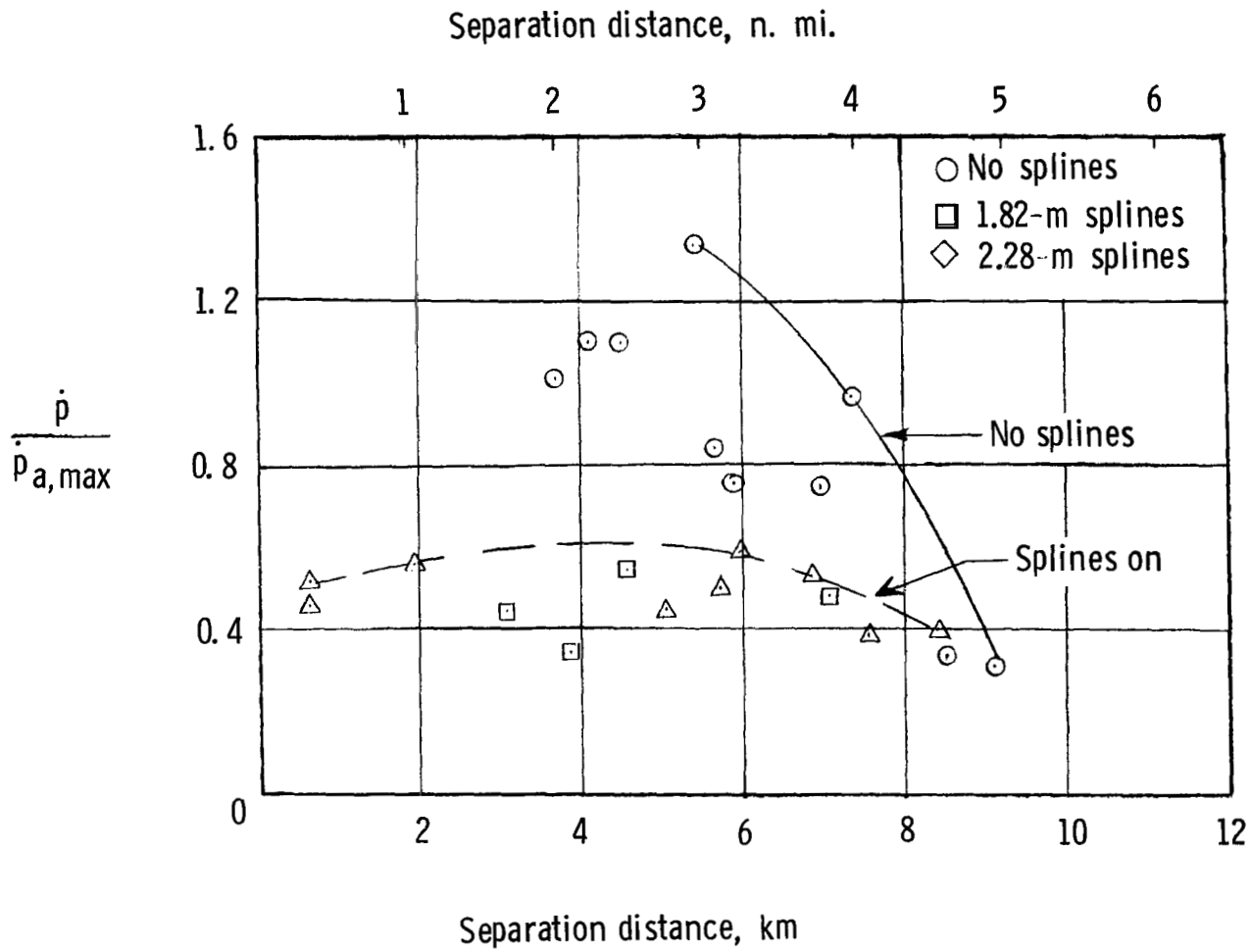

Figure 11.- Comparison of probe aircraft roll acceleration in attenuated and unattenuated vortices.

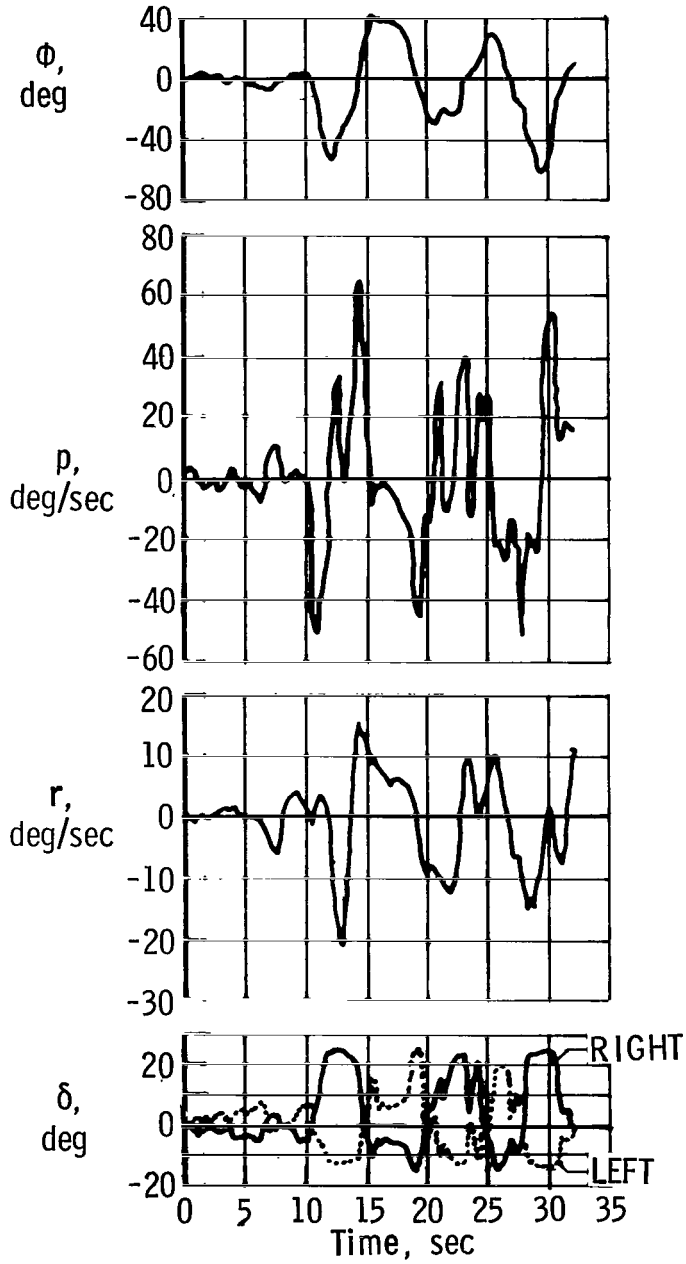

Figure 12.- Time history of penetration without splines at 4.06 km (2.19 n. mi.).

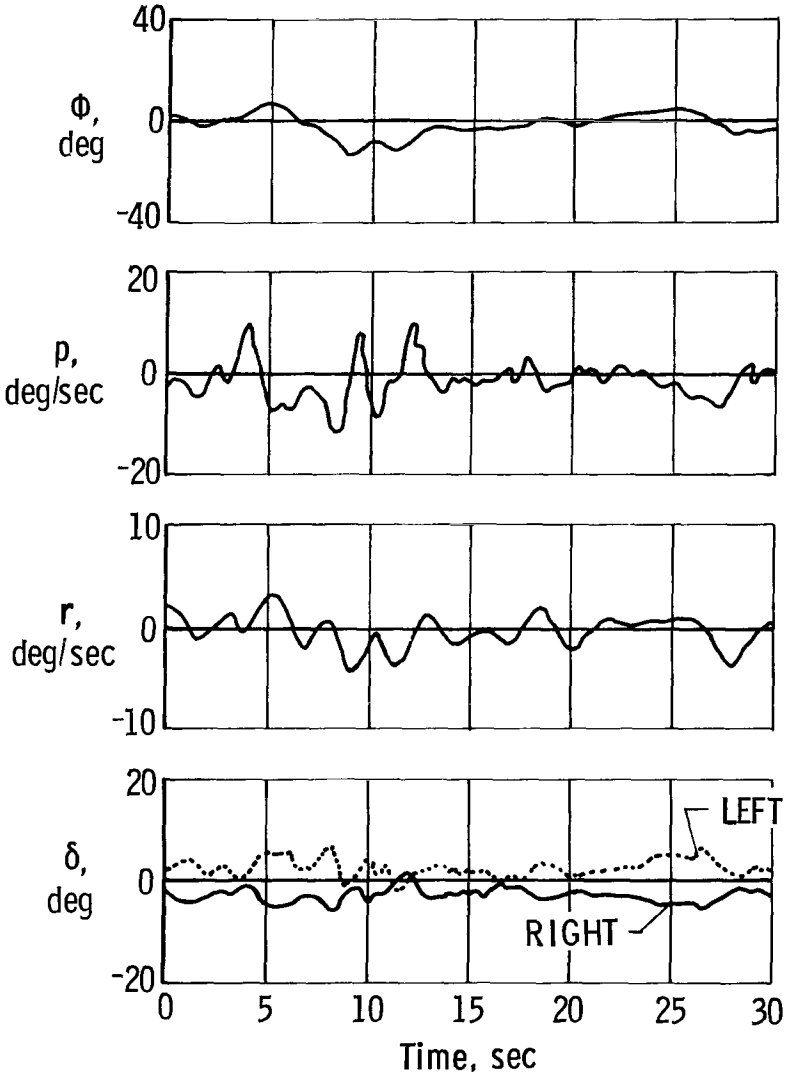

Figure 13.- Time history of penetration with splines at 1.56 km (0.84 n. mi.).

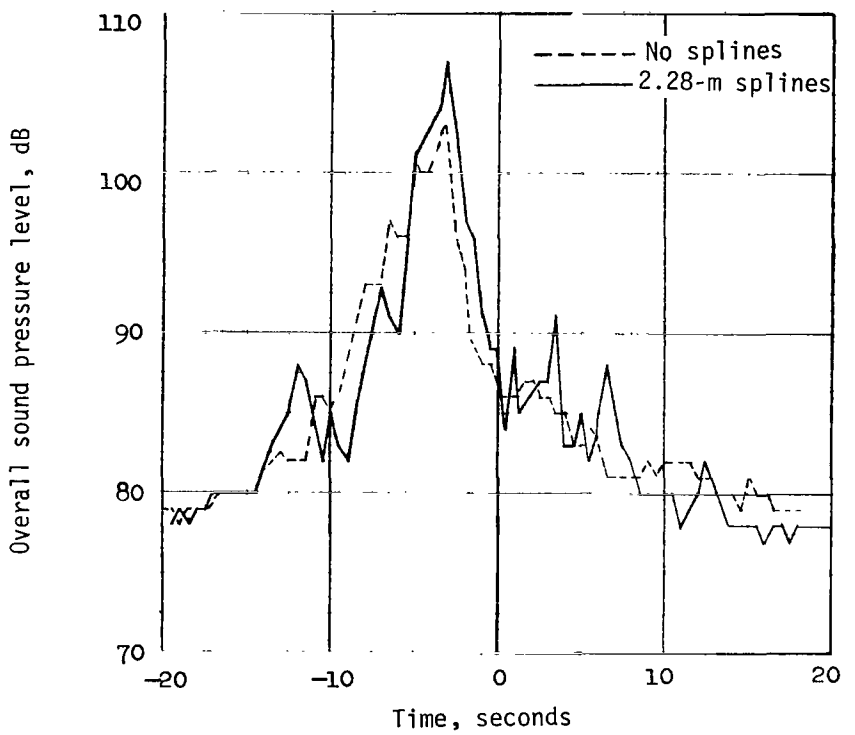

(a) Flyby: flaps and gear retracted.

Figure 14.- Typical maximum overall sound pressure level histories.

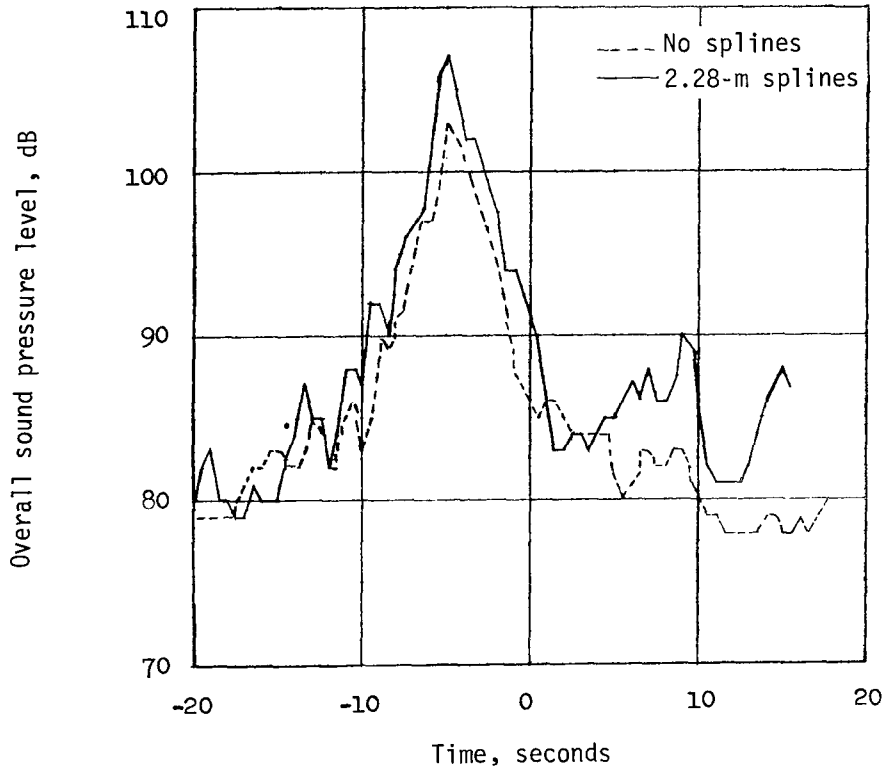

(b) Approach: gear down, flaps deflected 15^{o}.

Figure 14.- Concluded.

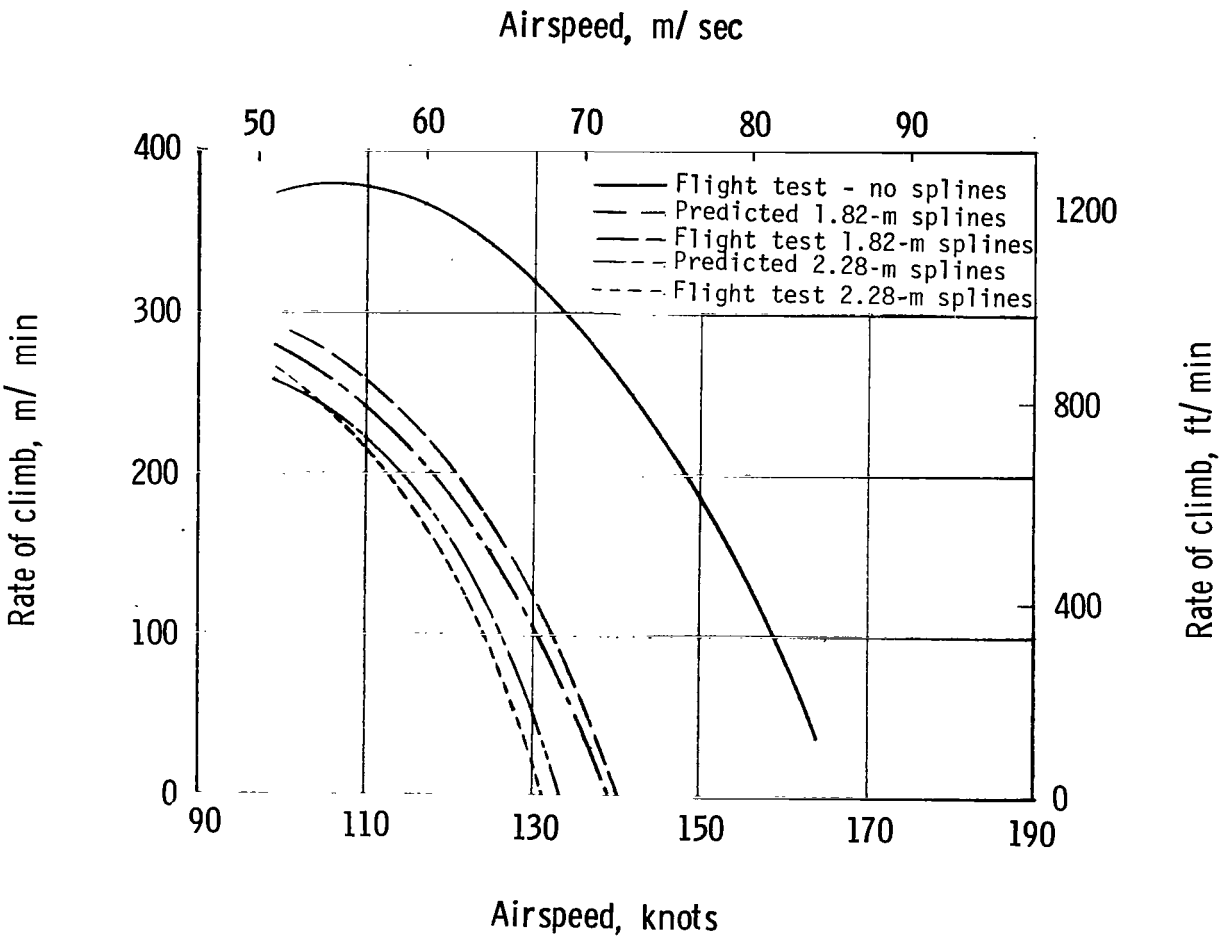

Figure 15.- Rate of climb for take-off configuration (gear down, 15° flaps) with maximum power of four engines.

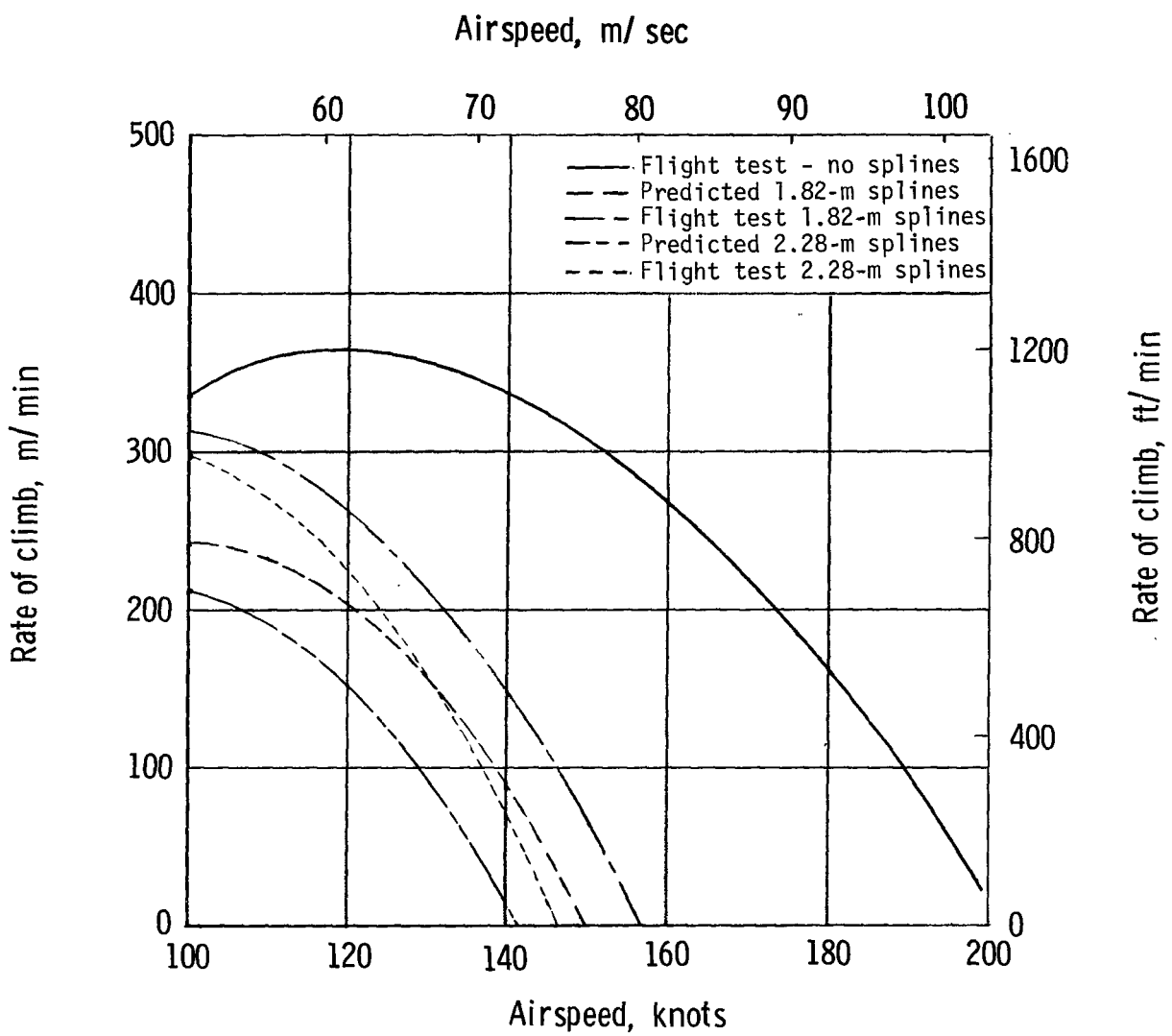

Figure 16.- Rate of climb for clean configuration (gear up, flaps up) with METO power of four engines.

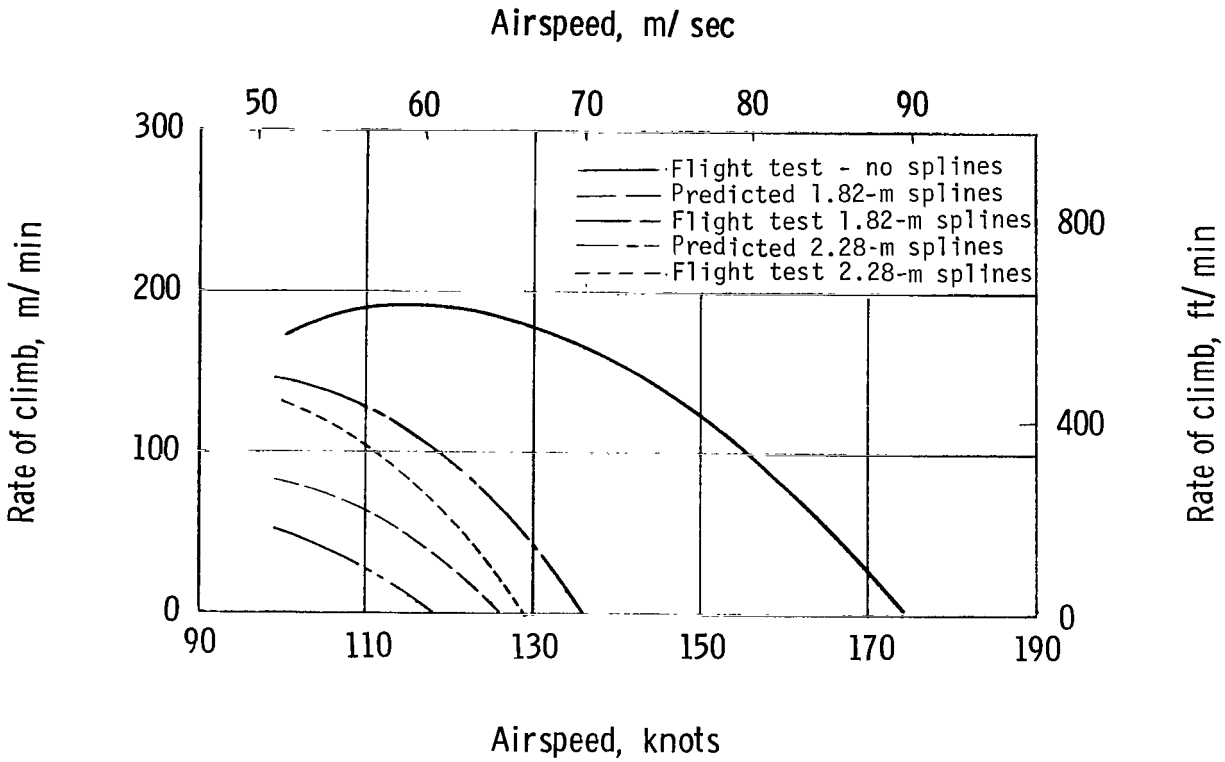

Figure 17.- Rate of climb for clean configuration (gear up, flaps up) with METO power and three engines and feathered propeller.

092 001 C1 U A 751128 S00903DS
DEPT OF THE AIR FORCE
AF WEAPONS LABORATORY
ATTN: TECHNICAL LIBRARY (SUL)
KIRTLAND AFB NM 87117

POSTMASTER: If Undeliverable (Section 158 Postal Manual) Do Not Return

"The aeronautical and space activities of the United States shall be conducted so as to contribute . . . to the expansion of human knowledge of phenomena in the atmosphere and space. The Administration shall provide for the widest practicable and appropriate dissemination of information concerning its activities and the results thereof."

—NATIONAL AERONAUTICS AND SPACE ACT OF 1958

NASA SCIENTIFIC AND TECHNICAL PUBLICATIONS

TECHNICAL REPORTS: Scientific and technical information considered important, complete, and a lasting contribution to existing knowledge.

TECHNICAL NOTES: Information less broad in scope but nevertheless of importance as a contribution to existing knowledge.

TECHNICAL MEMORANDUMS: Information receiving limited distribution because of preliminary data, security classification, or other reasons. Also includes conference proceedings with either limited or unlimited distribution.

CONTRACTOR REPORTS: Scientific and technical information generated under a NASA contract or grant and considered an important contribution to existing knowledge.

TECHNICAL TRANSLATIONS: Information published in a foreign language considered to merit NASA distribution in English.

SPECIAL PUBLICATIONS: Information derived from or of value to NASA activities. Publications include final reports of major projects, monographs, data compilations, handbooks, sourcebooks, and special bibliographies.

TECHNOLOGY UTILIZATION PUBLICATIONS: Information on technology used by NASA that may be of particular interest in commercial and other non-aerospace applications. Publications include Tech Briefs, Technology Utilization Reports and Technology Surveys.

Details on the availability of these publications may be obtained from:

SCIENTIFIC AND TECHNICAL INFORMATION OFFICE

NATIONAL AERONAUTICS AND SPACE ADMINISTRATION

Washington, D.C. 20546